Impact of Soil Moisture and Vegetation Water Content on Backscatter Simulated by WCM at Different Radar Parameters in Maize Field

Ge GAO

Abstract

This paper analysis the effects of soil moisture and vegetation water content (VWC) on total backscattering (σ_{tot}^0) simulated by water cloud model (WCM) throughout a growth cycle of maize at different frequencies, polarization modes, and incidence angles. Firstly, the bare soil backscatter (σ_{soil}^0) was simulated by Integral Equation Method (IEM) surface scattering model [1] or Dubois empirical backscattering approach [2]. Then, to analysis the effect of vegetation cover, a standard and a double layer WCM based on parameter sets of three published studies [3]-[5] are applied in this study area to simulate the two components of σ_{tot}^0, direct backscatter from vegetated surface (σ_{veg}^0) and attenuated soil backscatter ($\gamma^2\sigma_{soil}^0$). The input parameters of IEM, Dubois and WCM are supported by a series of ground measurements performed in Florida during the entire growth season, which includes soil moisture, surface roughness and vegetation biomass measurement. According to the analysis at different frequency and incident angle, the increase of bulk VWC can lead to either an increase or decrease in σ_{tot}. The different impact is determined by either σ_{veg}^0 or $\gamma^2\sigma_{soil}^0$ is the main contributor to σ_{tot}^0. At higher frequencies and larger incident angles, where the dominant part is from σ_{veg}^0, σ_{tot}^0 will increase with increasing bulk VWC. While, when $\gamma^2\sigma_{soil}^0$ becomes the main contributor to σ_{tot}^0, increasing bulk VWC leads to a denser canopy and thus more incoming microwave is attenuated. Therefore, increasing bulk VWC results in a decrease in σ_{tot}^0. Besides, according to the results obtained at C-band, different incident angle, HH-polarized microwaves are more sensitive to changes in bulk VWC, especially at larger incident angle. VV-polarization is less affected by vegetation cover, σ_{tot}^0 is sensitive to soil moisture even at peak biomass and large incidence angles, which is attributed to scattering along the soil-vegetation pathway.

Key Word: Water-cloud model, vegetation water content, radar backscatter coefficient, sensitivity analysis, time series analysis

I. Introduction

For bare soil, radar backscattering signals are sensitive to soil moisture variation, therefore, in recent years, with the development of space-borne synthetic aperture radar applications, many successful retrieval studies have been carried out [6, 7]. However, the backscattering coefficient of radar is not only affected by soil moisture, but also influenced by soil texture and surface roughness property. Roughness is characterized by two parameters: root mean square (RMS) value of height (s) and correlation length (l) [8, 9]. If the surface roughness property is not correctly represented or even not considered in the retrieval model, the accuracy of the model output will be greatly reduced. Therefore, a better model needs to describe s and l appropriately, the Integral Equation Method (IEM) surface scattering model was, thus,

developed. This model integrates backscatter signal which all comes from one complex surface and in this way, IEM is more in line with the backscatter of the actual surface and is widely used [1][10].

For vegetated surface, radar backscatter comprises contributions of direct backscatter from the vegetation, backscatter from the soil that is attenuated by the canopy and backscatter due to interactions between the vegetation and the underlying soil [11]. Therefore, one of the challenges for soil moisture retrieval at the vegetated surface is correcting the effects of vegetation cover [4]. Different semi-empirical and empirical methods have been carried out. In some retrieval models, the effects of vegetation are described explicitly [12, 13]. However, this increase the complexity of the model. Thus, other methods treat the effects of vegetation cover as constant during specific time intervals [14, 15]. This assumption also has its limitation, the application of the change detection approaches is, thus, applicable to regions with sparse vegetation or to time intervals with limited vegetation cover. Therefore, in order to get a robust soil retrieval model over different study areas with large variations on vegetation biomass, a better understanding of vegetation effects on σ_{tot}^0 is important.

In this paper, we discuss the effect of VWC on simulated σ_{tot}^0 for different frequencies, polarization modes, and incidence angles. A detailed ground measurement took place to support the simulation of σ_{soil}^0 and σ_{tot}^0, which includes soil moisture and vegetation biomass measurements in North Central Florida between April 27 and June 13, 2018, the detail of ground measurement will be introduced in the following section. A standard and a double layer WCM based on parameter sets of three published studies [3]-[5] are applied in this study area to simulate the σ_{tot}^0. In some studies, σ_{soil}^0 was simulated by the linear model based on their ground measurement [3, 5]. Considering the influence from different soil roughness condition, σ_{soil}^0 in our research are simulated by the Dubois empirical approach [2] instead, other parameters in WCM based on [3, 5] are not changed. σ_{soil}^0 in WCM at C-band is simulated by IEM according to [4]. Further, sensitivity and time series analysis are applied, the impact of soil moisture, bulk VWC and radar parameters on backscatter is discussed.

II. Measurements

A. Study Site

The ground measurement of this paper was conducted at the University of Florida Plant Science Research and Education Unit, located in North Central Florida near Citra, FL, USA. Sweet corn was planted in the field with 94.25% sand and 3.5% clay. The roughness property was measured in field, s = 0.94 cm, l = 15.189 cm. This research uses the observations through the entire growth period from 2018-4-27 to 2018-06-13.

B. Ground Measurement

1) Soil Moisture

Soil moisture is monitored continuously by the in-situ soil moisture network through the entire growth season. For this study, we used soil moisture at 5 cm.

2) VWC

The VWC was measured 4 times per week during the experiment. The measurement schedule is Monday at 6 A.M. Wednesday at 6 A.M and 6 P.M. Friday at 6 A.M from April 27 to June 13, 2018. Destructive sampling was performed. The samples will be weighted, both fresh and

after drying in the oven at 60°C for 48 hours. VWC values were determined from the difference between fresh and dry by the following equation:

$$VWC = \eta * \left[\left(m_{f,l} - m_{d,l}\right) + \left(m_{f,s} - m_{d,s}\right)\right] \qquad (1)$$

where η is the number of plants per square meter, and the superscripts l and s indicate leaves and stalks. The VWC was interpolated at the day without measurements.

III. Methodology

A. IEM

Before analyzing vegetated surface, the bare soil backscatter without vegetation effect must be analyzed. One of the methods use in this paper is semi-empirical IEM surface scattering model, which simulates the σ^0_{soil} of bare surfaces using parameterizations for the dielectric properties and the surface geometry. This method assumes the backscattering coefficient is only related to the incident angle, wave frequency, soil roughness and soil dielectric constant. In IEM, the soil dielectric constant is determined by soil type and soil moisture.

The surface roughness property is represented by s and l in IEM, which were measured at the ground measurement. In the following analysis, s and l are assumed to be constant and used to simulate the bare soil backscatter component for the entire growth period. The assumption that stable s and l at certain time interval is frequently adopted for soil moisture retrieval applications [15, 16, 17]

B. Dubois Empirical Backscattering Approach

According to the published studies, *Dabrowska-Zielinska et al. (2007)* and *Ulaby et al. (1984)* found the linear relation between soil moisture and σ^0_{soil}. This relation is based on their ground measurement. Therefore, in this paper, use Dubois empirical backscattering approach to simulate σ^0_{soil}. The algorithm is optimized for bare surfaces and requires two co-polarized channels at a frequency between 1.5 and 11 GHz [2]. The equation of this method is listed below:

$$\sigma^0_{hh} = 10^{-2.75} * \frac{cos^{1.5}\theta}{sin^5\theta} * 10^{0.028\epsilon*tan\theta}(khsin\theta)^{1.4} * \lambda^{0.7} \qquad (2)$$

$$\sigma^0_{vv} = 10^{-2.35} * \frac{cos^3\theta}{sin^3\theta} * 10^{0.046\epsilon*tan\theta}(khsin\theta)^{1.1} * \lambda^{0.7} \qquad (3)$$

C. Water-Cloud Model

Since the dielectric constant of dry vegetation is much smaller than the dielectric constant of water (usually several orders of magnitude), and the vegetation canopy generally has more than 99% of air in volume. WCM assumes that the canopy "cloud" contains uniformly distributed N water droplets, which the summation of N droplets equals to the water content of the canopy [18]. This model is a zeroth-order radiative transfer solution. The backscattered power from the entire canopy is divided into contributions from the canopy and underlying soil. However, backscattered power from the multiple scattering is neglected [11].

In this study, parameter sets developed from three published papers are used to build the forward WCM model in our case study area, each of which differs slightly form the original WCM in [18]. σ_{veg}^0 and $\gamma^2 \sigma_{soil}^0$ are two components in WCM, they are calculated separately to allow further comparison between different frequencies, incident angles and polarization modes. σ_{veg}^0 is determined according to different published studies. σ_{soil}^0 based on *Dabrowska-Zielinska et al.* [3] and *Ulaby et al.* [5] is simulated by empirical model build by *Dubois et al.* [2], the reason is stated above. And the σ_{soil}^0 based on *Joseph et al.* [4] is simulated by IEM [1].

1) C-band (VV, 23°) and L-band (HH, 35°)

Dabrowska-Zielinska et al. [3] developed a simplified WCM. In this method σ_{tot}^0 is described as

$$\sigma_{tot}^0 = \sigma_{veg}^0 + \gamma^2 \sigma_{soil}^0 \qquad (4)$$

One component is direct backscatter from vegetation, the other is backscatter from soil times the two-way attenuation γ^2. Further, σ_{soil}^0 is calculated with Dubois empirical method with (2) and (3), γ^2 and σ_{veg}^0 can be calculated with

$$\gamma^2 = \exp\left(\frac{-2BV_2}{cos\theta}\right) \qquad (5)$$

$$\sigma_{veg}^0 = AV_1^E cos\theta * (1 - \gamma^2) \qquad (6)$$

A, B and E are model parameters which are listed in table 1, θ is incident angle, V_1 and V_2 are vegetation parameters used to represent the canopy. In this report, V_1 and V_2 are represented by bulk VWC [3].

2) C-band (HH- and VV-polarization with different incident angles)

Joseph *et al.* [5] calibrated their model for C-band backscatter with co-polarization at 15°, 35°, 55° respectively. The parameter set for different polarization modes and angles are listed in table 1. Here the σ_{tot}^0 is also calculated by (4). Further, σ_{veg}^0 and γ^2 are calculated with (7) and (8), σ_{soil}^0 is simulated by IEM.

$$\gamma^2 = \exp\left(\frac{-BV_2}{cos\theta}\right) \qquad (7)$$

$$\sigma_{veg}^0 = (1 - \gamma^2) * AV_1 cos\theta \qquad (8)$$

Here, V_1 and V_2 are represented by bulk VWC [4].

3) X-band (VV-polarization with 50° incident angle)

Ulaby et al. [5] divided the σ_{veg}^0 into two parts. One part is the backscattered power by leaf layer and the other is by stalk layer. Thus σ_{tot}^0 is described as

$$\sigma_{tot}^0 = \sigma_{leaf}^0 + \sigma_{stalk}^0 + \gamma^2 \sigma_{soil}^0 \qquad (9)$$

Then, σ_{soil}^0 is calculated with (3) and σ_{lef}^0, σ_{stalk}^0 are described as

$$\sigma^0_{leaf} = A_{leaf}\left[1 - \exp\left(\frac{-B_{leaf}V_1}{h_1}\right)\right] * (1 - \gamma^2_{leaf})cos\theta \qquad (10)$$

$$\sigma^0_{stalk} = A_{stalk} * V_2 * \frac{h_2}{h} * \gamma^2_{leaf} \qquad (11)$$

Parameters related to leaf layer are A_{leaf}, B_{leaf}, leaf layer height h_1 and leaf attenuation factor γ^2_{leaf}. Parameter related to stalk layer are A_{stalk}, height of stalk layer h_2. Other parameters are total plant height h and incident angle θ. In this report, h is the measured maximum plant height, h_2 is the height of the lowest leaf, and h_1 is calculated by $h - h_2$. Further, the attenuation factors are described as

$$\gamma^2_{leaf} = \exp(-2 * \alpha_{leaf} * sec\theta V_1) \qquad (12)$$

$$\gamma^2_{stalk} = \exp\left(-\alpha_{stalk} * V_2 * \frac{h_2}{h}\right) \qquad (13)$$

Where α_{leaf} and α_{stalk} are parameters listed in table 1. In this research, parameter V_1 and V_2 are vegetation parameters that are used to describe the canopy. Here, we first use leaf water content represent V_1 and stalk water content represent V_2. Then, we use leaf area index (LAI) represent V_1 and stalk water content for V_2. Equation (9-13), which were also used by *Tim et al.* [19] to estimate the total backscatter in maize field, are slightly different from the original *Ulaby's* paper.

Table 1

Parameters used in Water-Cloud Model

Model		Radar Parameter					Vegetation Parameter				
	Band	Freq.(GHz)	Pol.	$\theta(^o)$	A		B	α_{lef}	E	A_{st}	α_{st}
Ulaby *et al.* (1984)	X	9.6	VV	50	0.218		0.56	0.411		0.025	0
Dabrowska-Zielinska *et al.* (2007)	L	1.3	HH	35	0.011		0.043	2.9038			
	C	5.3	VV	23	0.0795		0.1464	0			
Joseph *et al.* (2010)	C	5.3	HH	15	0.03		0.09				
	C	5.3	VV	15	0.01		0.13				
	C	5.3	HH	35	15.96		$1.18 * 10^{-4}$				
	C	5.3	VV	35	3.05		$1.38 * 10^{-4}$				
	C	5.3	HH	55	5.57		$4.16 * 10^{-4}$				
	C	5.3	VV	55	2.96		$1.96 * 10^{-4}$				

IV. Result and discussion

A. VWC

The VWC is shown in Figure 1, this figure shows the bulk VWC, stalk and leaves VWC respectively. With the growth of the maize, the major part of water in the plant is stored in the stem. Thus, the trend and variation of bulk and stem VWC are very similar, this variation is influenced by the growing situation in the field like irrigation and precipitation etc. From 2018-05-25 to the end of the growth season, the leaves VWC is quite stable. Dielectric property of

vegetation depends largely on the water, and the other factors like salinity and water temperature has less influence [11].
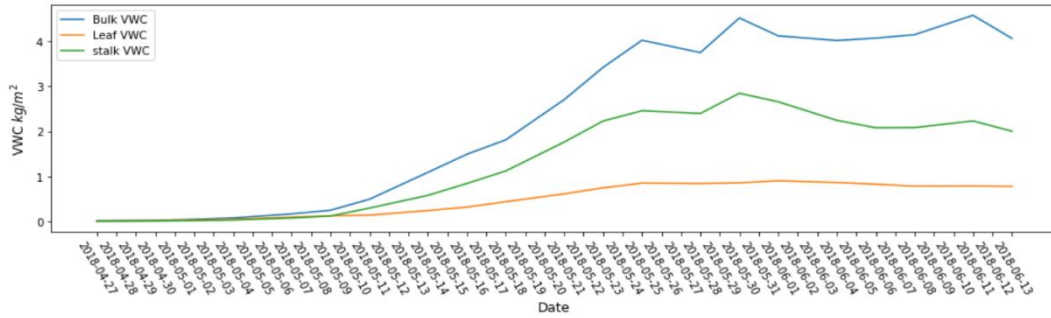

Figure 1 Variation of VWC during the entire growth period

B. Backscatter sensitivity study

1) Dabrowska-Zielinska et al. (2007):

In this section, use Dubois model simulate the bare soil backscatter. Then, for WCM, use parameter set by *Dabrowska-Zielinska et al.* listed in table 1 to simulate the total backscatter. Figure 2 shows the result of horizontally co-polarized (HH) backscatter at 1.3GHz and incident angle of 35°.
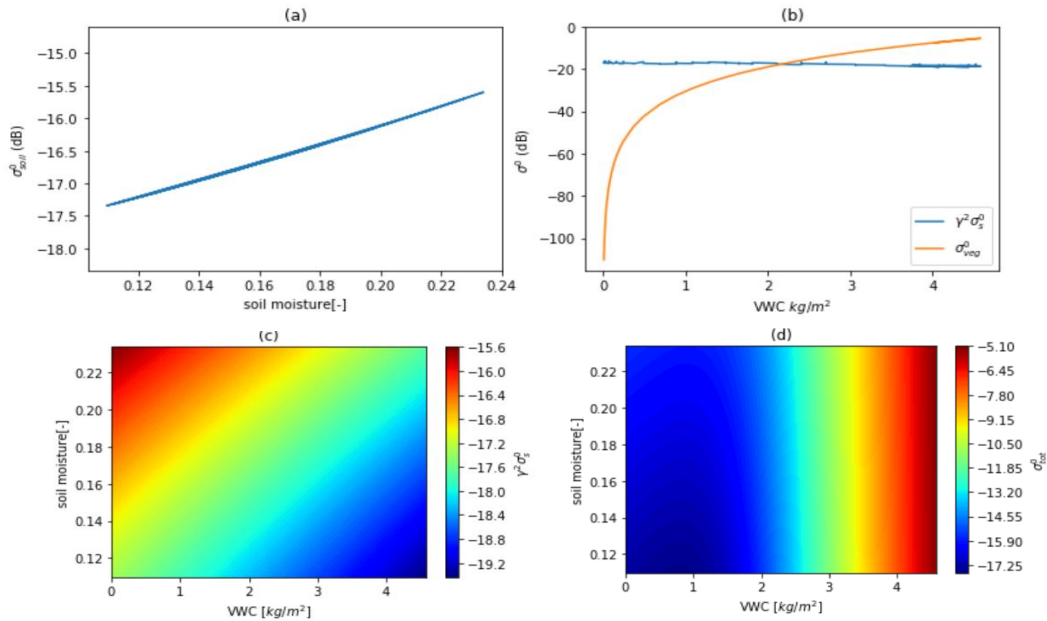
Figure 2 *Sensitivity of L-band (1.3 GHz, HH, 35 ∘) radar backscatter modeled using Dabrowska-Zielinska* et al. *[3] to soil moisture and bulk VWC. (a) Soil backscatter as function of soil moisture. (b) Vegetation backscatter as function of bulk VWC, including the range of the attenuated soil backscatter contribution. (c) Attenuated soil backscatter as function of bulk VWC and soil moisture. (d) Total backscatter as function of bulk VWC and soil moisture.*

The variation of bare soil backscatter is in the range around 1.7 dB with the soil moisture change from 0.11 to 0.23 m^3/m^3 (see in Figure 2(a)). With the increasing soil moisture, the attenuated soil backscatter increases and changes in the range around 1.6 dB. The bulk VWC changes from 0 to 4.6 kg/m^2, with increasing bulk VWC, the attenuated soil backscatter decreases and

changes in the range around 2.4 dB. Besides, with larger bulk VWC, attenuated soil backscatter is less sensitive to soil moisture (see in Figure 2(c)). Meanwhile, during the growth period, the variation of vegetation backscatter is way larger than the attenuated soil backscatter (see Figure 2(b)), the backscatter of attenuated soil and vegetation are equal around bulk $VWC = 2 \text{ kg}/m^2$. When the bulk VWC is larger than 2 kg/m^2, the total backscatter simulated by this WCM is primarily sensitive to the variation of bulk VWC. Besides, with increasing bulk VWC, the value of total backscatter increases, which indicates the main contribution to total backscatter is made by direct vegetation backscatter (see in Figure 2(d)).

According to the observation from Figure 2, the bulk VWC contributes to large part of the simulated total backscatter, changes in soil moisture has small effect. With increasing bulk VWC, the total backscatter increases, the transparency of the canopy layer decreases, thus, more soil backscatter is attenuated. According to previous study, lower frequency, small incidence angles (5 - 15° from nadir), HH polarization is best suited for soil monitoring [20]. In this case, L-band, HH-polarization and 35° incident angle, large incident angle increase the path through the canopy layer. Therefore, changes in soil moisture cannot play the main role in the simulation of total backscatter. Although, L-bend has deeper penetration ability, with higher incident angle and small soil moisture, total backscatter simulated by this WCM is more sensitive to the variation in VWC.
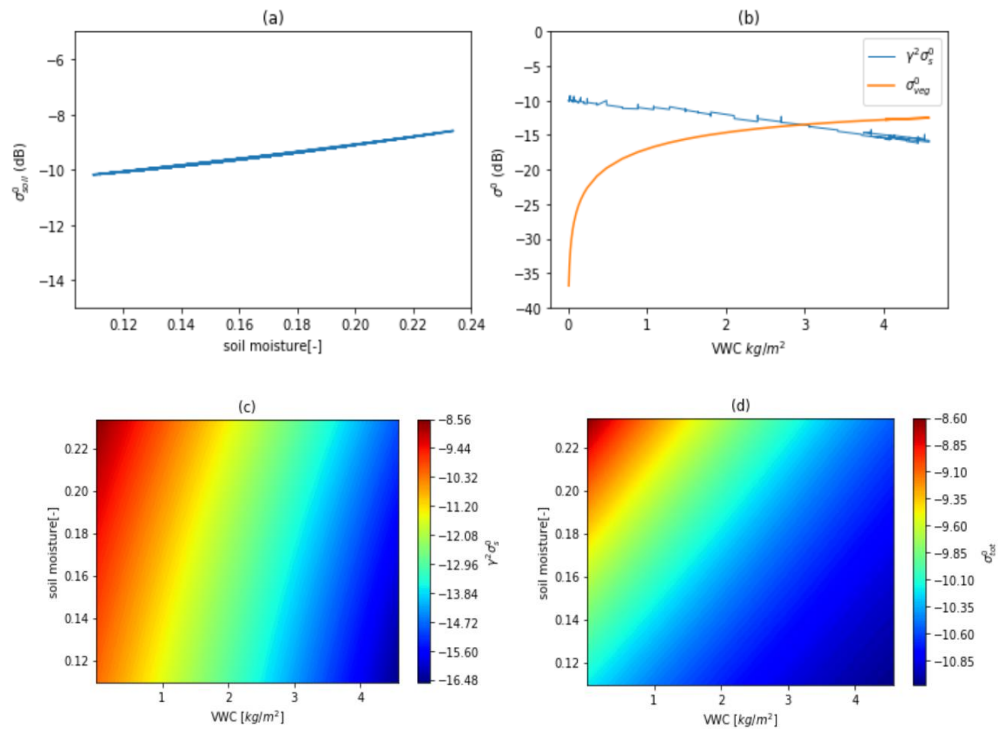

Figure 3 Sensitivity of C-band (5.3 GHz, VV, 23◦) radar backscatter, using Dabrowska-Zielinska et al. [3], to soil moisture and bulk VWC. (a) Soil backscatter as function of soil moisture. (b) Vegetation backscatter as function of bulk VWC. (c) Attenuated soil backscatter as function of bulk VWC and soil moisture. (d) Total backscatter as function of bulk VWC and soil moisture.

The result of 5.3 GHz, VV-polarization, incidence angel of 23° is shown in Figure 3. Bare soil backscatter is simulated by Dubios model, and the parameter sets used in WCM is listed in table 1. The bare soil soil backscatter changes in the range around 1.6 dB with the soil moisture varies

from 0.11 to 0.23 m^3/m^3 (see in Figure 3(a)). With the increasing soil moisture, the attenuated soil backscatter increases and changes in the range around 2.64 db. The bulk VWC changes from 0 to 4.6 kg/m^2, with increasing bulk VWC, the attenuated soil backscatter decreases and changes in the range around 5.28 dB (see in Figure 3(c)). Meanwhile, during the growth period, the variation of vegetation backscatter and attenuated soil backscatter is in the comparable magnitude (see Figure 3(b)). Therefore, the total backscatter is sensitive to both soil moisture and bulk VWC (see Figure 3(d)). And the backscatter of attenuated soil and vegetation are equal around bulk VWC = 3 kg/m^2 (see Figure 3(b)). When the bulk VWC is smaller than 3 kg/m^2, the total backscatter simulated by this WCM is more sensitive to variation of soil moisture, while when VWC is larger than 3 kg/m^2, the variation of soil moisture has smaller impact. Moreover, with increasing bulk VWC value, the total backscatter decreases, which means the main contribution to total backscatter is made by attenuated soil backscatter (see in Figure 3(d)).

In this case, the path through the canopy layer is smaller with a smaller incidence angle. The microwave can have better penetration ability. Therefore, less soil backscatter is attenuated by vegetation. Thus, change in the soil moisture has obvious influence on the simulated total backscatter. However, this influence becomes weaker with the increasing bulk VWC, because higher VWC makes the canopy layer less transparent to microwave.

2) A.T Joseph et al. (2010):

In this section, results are displayed in C-band, co-polarization mode with three different incident angles (15°, 35°, 55° respectively). The total backscatter is simulated based on Joseph et al. (2010). In this method, bare soil backscatter is simulated by IEM model and the parameter set used in the WCM is listed in table 1.

In figure 4, the result shows vertically co-polarized backscatter simulated at incidence angle of 15°, 35°, 55° respectively. Both soil moisture and bulk vegetation varies in the range which was observed during the growth period.

From Figure 4(a - c), the variation of vegetation backscatter has similar trend which increases with increasing bulk VWC. At 15°, σ^0_{veg} increase from -69.8 dB to -16.9 dB. At 35°, σ^0_{veg} increase from -74.7 dB to -20.5 dB. At 55°, σ^0_{veg} increase from -73.3 dB to -19.1 dB. σ^0_{veg} is smaller when incident angle is 15°, the difference between 15° and larger angle can up to 5 dB.
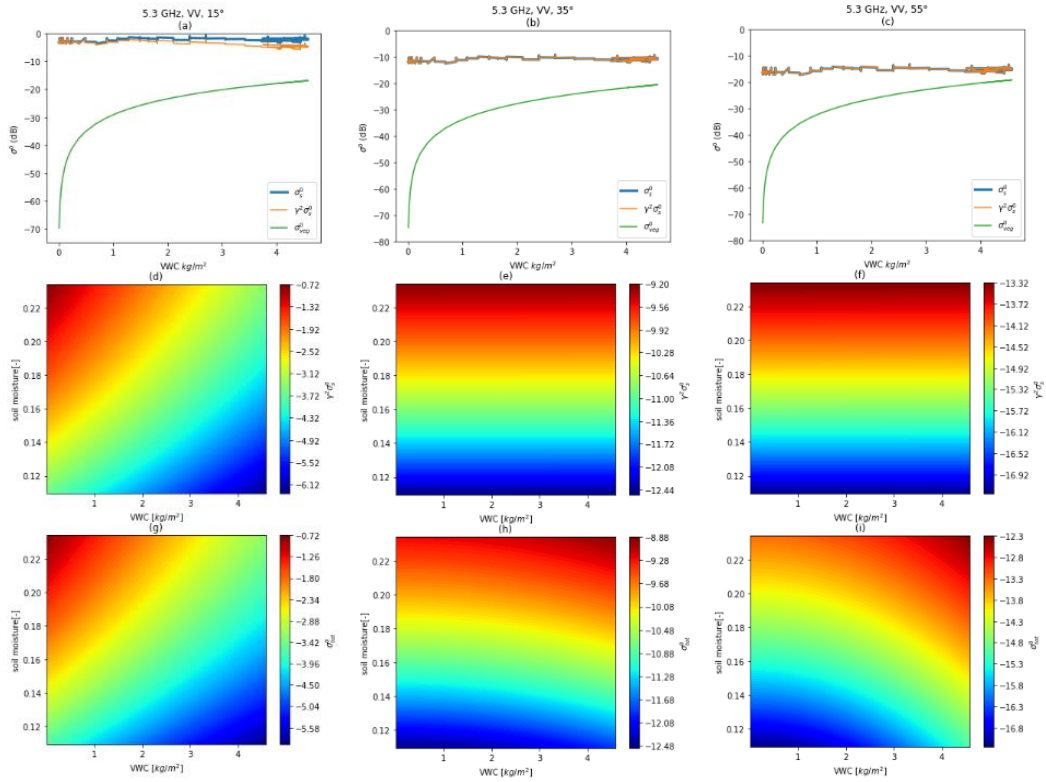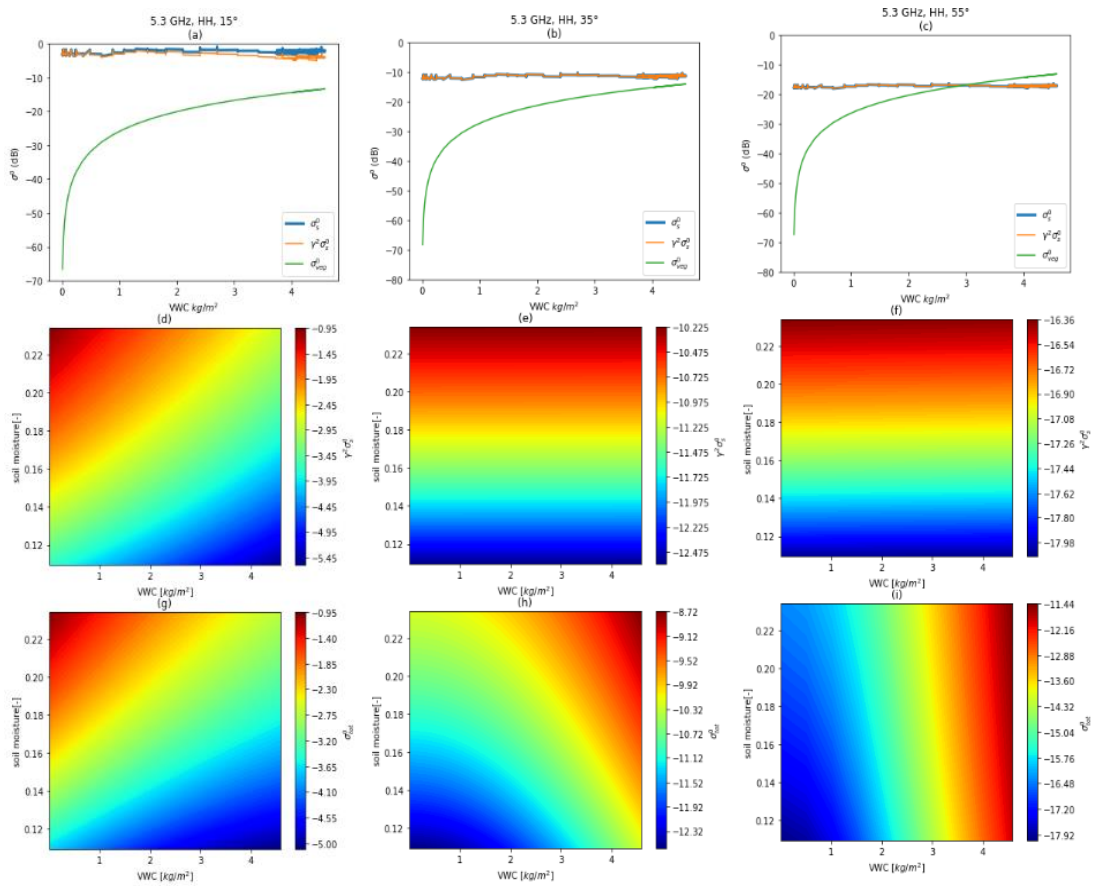
Figure 4 Sensitivity of C-band (5.3 GHz) vertically polarized radar backscatter at different incidence angles using Joseph et al. [4]. (a)–(c) Vegetation and attenuated soil contributions as a function of bulk VWC for 15°, 35°, and 55°, respectively. (d)–(f) Attenuated soil backscatter as a function of bulk VWC and soil moisture for 15°, 35°, and 55°, respectively. (g)–(i) Total backscatter as a function of bulk VWC and soil moisture for 15°, 35°, and 55°, respectively.

However, the difference between σ_{veg}^0 at 35° and 55° is within 1.5 dB. Thus, at small incident angle, the path through canopy layer is small and σ_{veg}^0 contributes less to the total backscatter. For $\gamma^2\sigma_{soil}^0$, which decreases from -1.5 dB to -5.8 dB, -9.2 dB to -12.5 dB, -13.3 dB to -17.2 dB at 15°, 35°, 55° with increasing bulk VWC respectively. Larger incident angle leads to longer path through canopy layer, thus the value of attenuated soil backscatter is smaller at larger angle. Meanwhile, in Figure 4 (d-f), at 15°, $\gamma^2\sigma_{soil}^0$ decreases considerably with increasing bulk VWC and still sensitive to soil moisture even at the largest bulk VWC. However, at 35° and 55°, $\gamma^2\sigma_{soil}^0$ is independent with bulk VWC, the reason is the parameter B used in the WCM. At larger incident angle, B value listed in table 1 is way smaller than B value at 15°. Then, γ^2 which is related to bulk VWC and B is close to 1. Thus, $\gamma^2\sigma_{soil}^0$ is independent with the variation of bulk VWC. However, larger bulk VWC makes the canopy layer more difficult to penetrate, this principle is valid no matter what incident angle is. Therefore, the value of B is too small in Joseph's WCM which leads to the failure of the model to capture the variation of attenuated soil backscatter due to bulk VWC variation. However, in Figure 4 (g-i), the influence of bulk VWC to total backscatter is obvious at larger incident angle, the reason is because the other parameter A is considerably larger at higher incident angle, which leads to higher vegetation backscatter. Besides, at 15°, attenuated soil backscatter is much larger than vegetation backscatter compared with other incident angles, which means attenuated soil backscatter provides the majority part of total backscatter. Therefore, with bulk VWC increases,

the total backscatter decreases (see in Figure 4(g)). At 35° and 55°, although the magnitude of vegetation and attenuated soil backscatter is comparable, attenuated soil backscatter remains the main contributor to total backscatter. However, at larger incident angle, the total backscatter increases with increasing bulk VWC, this trend is more obvious at 55° (see in Figure 4(h-i)).

In Figure 5, the result of C-band, horizontally co-polarization at incident angle of 15°, 35° and 55° respectively is shown. The result of HH- and VV- polarization is similar. Note that at 55°, the vegetation backscatter is larger than attenuated soil backscatter at bulk VWC around $3kg/m^2$. Compared with what we obtained at VV polarization mode, at HH-polarization mode, total backscatter is less sensitive to soil moisture variation, especially at larger incident angle.

Figure 5 Sensitivity of C-band (5.3 GHz) horizontally polarized radar backscatter at different incidence angles using Joseph et al. [4]. (a)–(c) Vegetation and attenuated soil contributions as a function of bulk VWC for 15°, 35°, and 55°, respectively. (d)–(f) Attenuated soil backscatter as a function of bulk VWC and soil moisture for 15°, 35°, and 55°, respectively. (g)–(i) Total backscatter as a function of bulk VWC and soil moisture for 15°, 35°, and 55°, respectively.

3)   Ulaby et al.(1984):

The result of backscatter is simulated based on Ulaby's WCM using (7)-(8). The result is shown in Figure 6. X-band with frequency of 9.6 GHz, vertically co-polarized with 50° incident angle. In this model, the vegetation backscatter is divided into stalk and leaf parts. In order to make the sensitivity plot of the two main influence factors (soil moisture and bulk VWC), assume the

leaf VWC is 0.33 of the bulk VWC (which is averaged over the growth period), the height of the leaf layer is 1.04 m (average over the growth period) and the height of the stalk layer over the total height is 0.07 (average over the growth season)
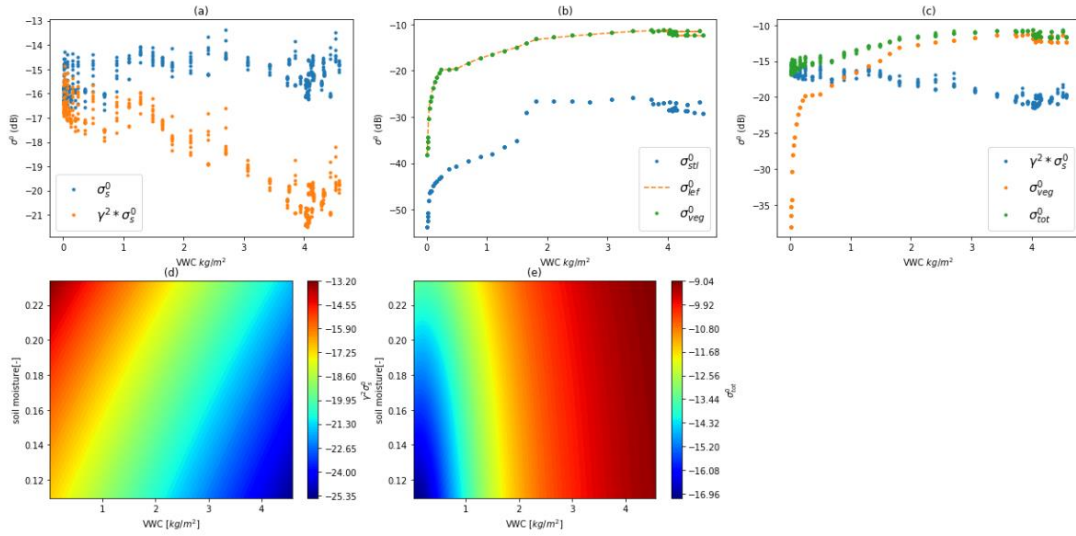

Figure 6 Sensitivity of radar backscatter at 9.6 GHz to soil moisture and bulk VWC using Ulaby et al. [5]. (a)–(c) different contributor of total backscatter as function of bulk VWC. (d) Attenuated soil backscatter as function of soil moisture and bulk VWC. (e) Total backscatter as function of soil moisture and bulk VWC.

.

At X-band, vegetation backscatter exceeds the attenuated soil backscatter at the bulk VWC around 1 kg/m^2, the soil part is important only if $VWC < 1 \, kg/m^2$. Compared with what we obtained at C-band, VV-polarization and 55° incident angle, in this case, the vegetation backscatter exceeds the attenuated soil backscatter at much lower bulk VWC value (see in Figure 6(c)). With bulk VWC increasing from 0 to $4.6 kg/m^2$, the attenuated soil backscatter decreases from -13.20 to -25.35 dB (see in Figure 6 (d)) and the influence is more obvious when bulk VWC larger than $1 kg/m^2$ (see in Figure 6(a)). Moreover, the main contributor of the vegetation backscatter is the backscatter from the leaf layer (see in Figure 6(b)).

With soil moisture increasing from 0.04 to $0.23 m^3/m^3$, the attenuated soil backscatter increases from -17.25 to -13.20 dB. Besides at larger bulk VWC, attenuated soil backscatter is less sensitive to soil moisture (see in Figure 6(d)). For the total backscatter, as shown in Figure 6(e), when the bulk VWC is smaller than 1 kg/m^2, total backscatter is influenced by both soil moisture and bulk VWC, but more sensitive to the change in bulk VWC. However, when the value of bulk VWC exceeds 1 kg/m^2, the variation of total backscatter is dominated by the variation in bulk VWC. Besides, with increasing bulk VWC value, total backscatter increases, which indicates that the main contribution to total backscatter is made by direct backscatter from vegetation.

C. Time series analysis
1) Dabrowska-Zielinska et al. (2007):

Figure 7 (a) shows σ_{tot}^0 simulated by WCM at L-band, 35° incident angle and HH polarization. Figure 8 (a) shows the total backscatter simulated by WCM at C-bend, 23° incident angle and VV polarization. The parameter set is derived by Dabrowska-Zielinska et al. (2007) and is listed
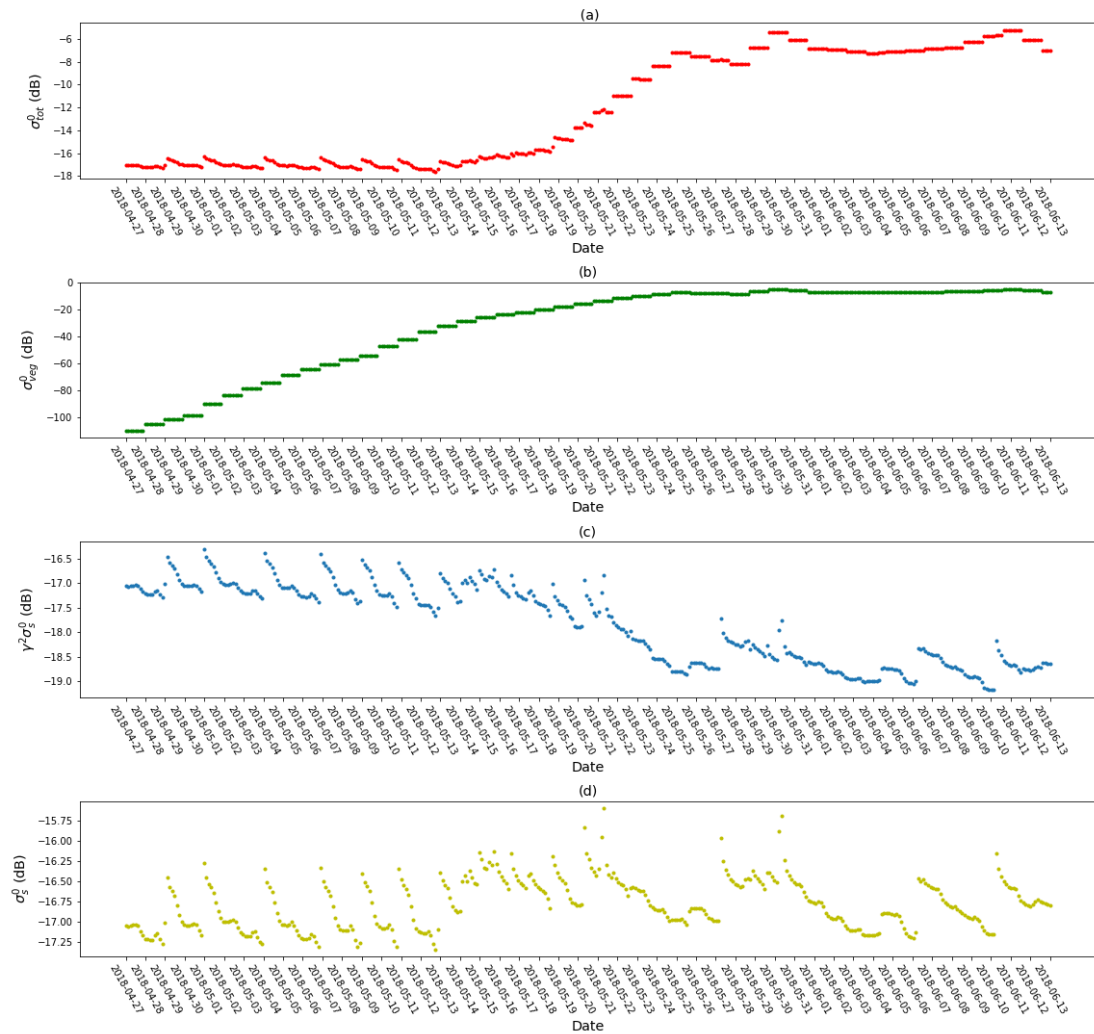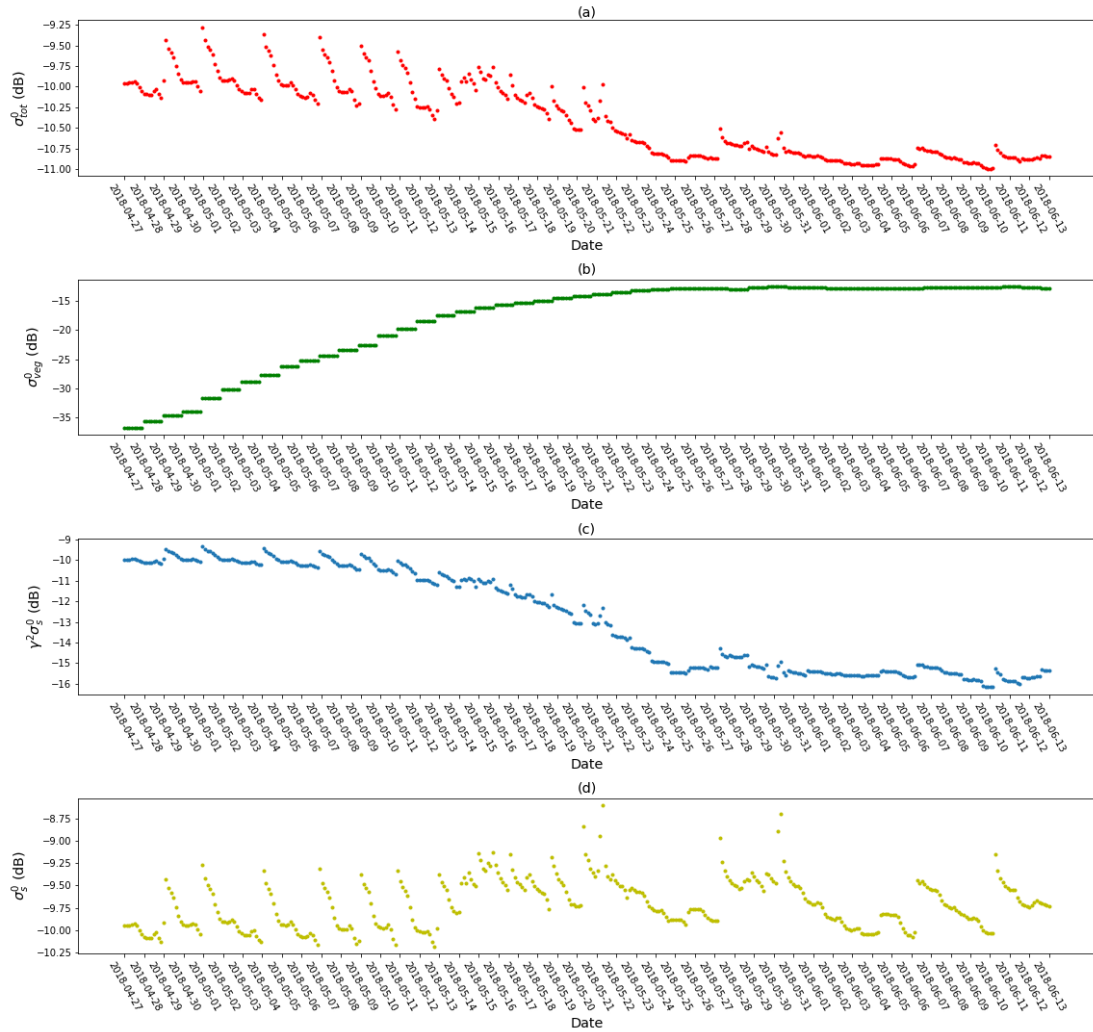

Figure 7 Modeled radar backscatter time series at L-band (1.3 GHz, HH, 35°) using Dabrowska-Zielinska et al. [3]: (a) total backscatter, (b) vegetation backscatter, (c) attenuated *soil backscatter, (d) bare soil backscatter.*

in table 1 as well. (b)-(c) plots in Figure 7 and Figure 8 show the individual parts of the total backscatter which are vegetation backscatter (σ_{veg}^0) and attenuated soil backscatter ($\gamma^2 \sigma_{soil}^0$) respectively. Plot (d) in Figure 7 and Figure 8 show the bare soil backscatter (σ_{soil}^0) simulated by Dubois method.

Figure 7 (d) is the soil backscatter without the influence of vegetation cover at L-band HH polarization with 35° incidence angle, σ_{soil}^0 varies in the range of -17.3 to -15.6 dB caused by soil moisture variation. Figure 7 (c) shows the impact of the variation in VWC on simulated attenuated soil backscatter. With the impact of VWC, $\gamma^2 \sigma_s$ is smaller than σ_s as expected and the difference between $\gamma^2 \sigma_{soil}^0$ and σ_{soil}^0 is in the range of 3.3 to 5.7 dB. In plot (b), the vegetation backscatter increases from -110.2 to -5.4 dB with increasing bulk VWC during the growth period. According to previous study, L-band has better ability to penetrate the canopy

layer and with increasing incident angles this ability decreases, thus, less sensitive to soil moisture [4,47,46]. Based on the result shown in Figure 7 (a), σ_{tot}^0 is mainly influenced by σ_{veg}^0 especially at the late growth period, the variation of σ_{tot}^0 shows less influence from $\gamma^2\sigma_{soil}^0$. Also, recall the sensitivity analysis result shown in Figure 2 (d). Therefore, in maize field, even L-band has better penetration ability, at HH polarization and 35° incident angle, the influence of σ_{veg}^0 cannot be neglected.

At C-band, VV polarization and 23° incident angle, σ_s in Figure 8 (d) varies in the range of -10.2 to -8.6 dB caused by soil moisture variation. Comparing plot (c) and (d) in Figure 8, the

Figure 8 Modeled radar backscatter time series at C-band (5.3 GHz, VV, 23°) using Dabrowska-Zielinska et al. [3]:

(a) total backscatter, (b) vegetation backscatter, (c) attenuated soil backscatter, (d) bare soil backscatter.

difference between $\gamma^2\sigma_{soil}^0$ and σ_{soil}^0 is in the range up to 6.3 dB. Besides, the value of σ_{veg}^0 is much bigger compared with what is shown in Figure 7 (b), especially at the beginning of the growth season. In Figure 8 plot (a), σ_{tot}^0 is primarily influenced by $\gamma^2\sigma_{soil}^0$. Therefore, in maize field, at C-band, VV polarization, with incident angle of 23°, the influence of σ_{veg}^0 is more obvious at late growth period, however, simulated σ_{tot}^0 is mainly dominated by $\gamma^2\sigma_{soil}^0$.

2)   A.T Joseph et al. (2010):

Figure 9 to Figure 11 show the time series of backscatter simulated by WCM derived by A.T Joseph et al. (2010) for C-band at different incidence angles (15°, 35°, 55°) and co-polarization, respectively. The value of simulated σ_{tot}^0 at VV polarization mode decreases with increasing incident angles. At 15°, the range of σ_{tot} is -5.5 dB to -1.6 dB. At 35°, the range of σ_{tot}^0 is -12.5 dB to -9.0 dB. At 55°, the range of σ_{tot}^0 is -17.2 dB to -12.4 dB. The same situation can be seen in HH polarization as well, the value of σ_{tot}^0 decreases with increasing incident angles. At 15°, the range of σ_{tot}^0 is -4.5 dB to -1.7 dB. At 35°, the range of σ_{tot}^0 is -12.5 dB to -8.8 dB. At 55°, the range of σ_{tot}^0 is -18.0 dB to -11.5 dB. At C-band, close to nadir, the variation of σ_{tot}^0 is mainly influenced by $\gamma^2 \sigma_{soil}^0$ At higher angles, bulk VWC influences the direct backscatter from vegetation, which is the main contribution to σ_{tot}^0. Moreover, the higher incident angle has a larger impact on $\gamma^2 \sigma_{soil}^0$ at HH-polarization.

At C-band, 15° incident angle, σ_{soil}^0 at HH and VV-polarization modes is simulated by IEM has similar value at the beginning of the growth period. Then, a higher σ_{soil}^0 value obtained at VV-polarization becomes more obvious as the plant grows (see in Figure 9 (d)). However, this difference is not big during the entire growth period, which is in the range of less than 0.2 dB.
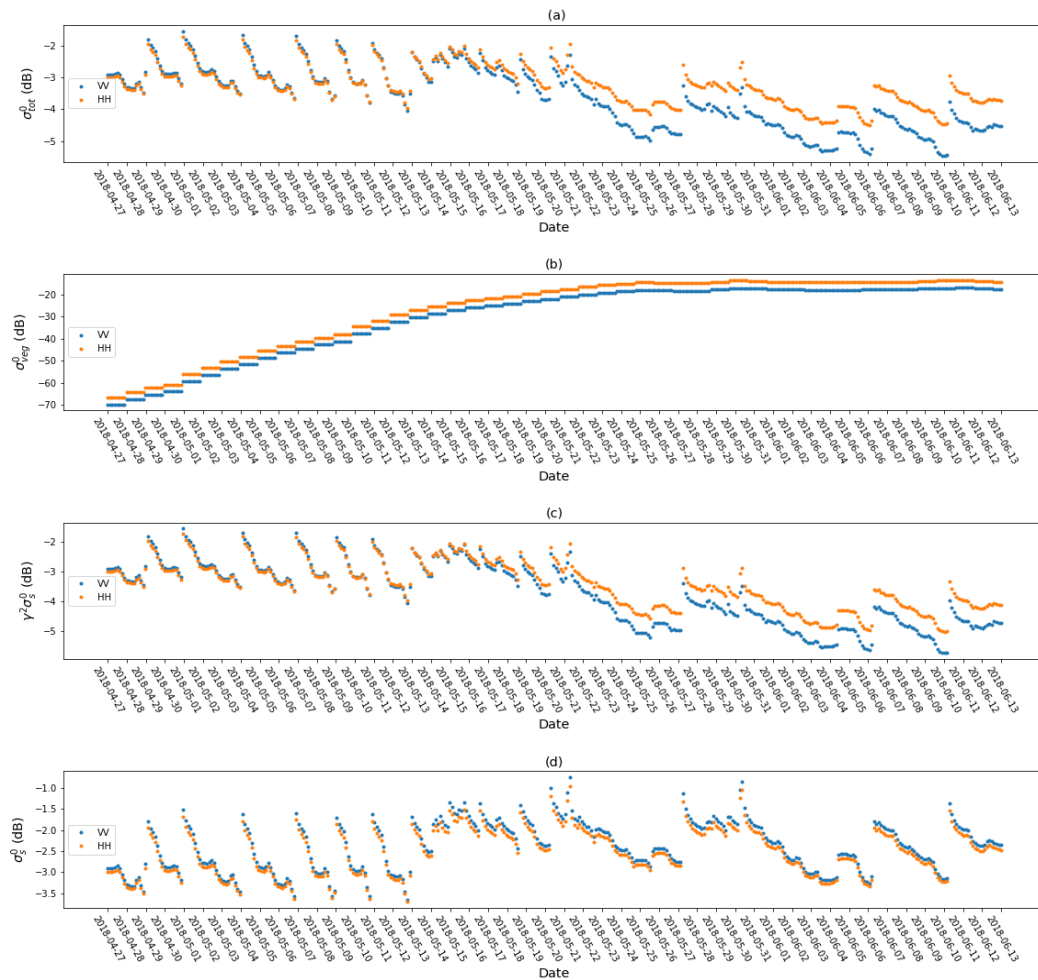

Figure 9 Modeled radar backscatter time series at horizontally and vertically polarized C-band (5.3 GHz) and 15°

incident angle using Joseph et al. [4]: (a) total backscatter, (b) vegetation backscatter, (c) attenuated soil backscatter,

(d) bare soil backscatter.

In Figure 9 (c), the difference between $\gamma^2\sigma_{soil}^0$ at HH and VV polarization is obvious around 2018-05-17 and becomes bigger as the plant grows, similar to σ_{soil}^0 The difference is in the range of up to 0.7 dB. Compare the plot (c) and (d), a large bulk VWC value has more impact on VV- than HH-polarization, which leads to a smaller $\gamma^2\sigma_{soil}^0$ value. The direct backscatter from vegetation shows an increasing trend during the entire growth period in both VV- and HH-polarization. σ_{veg}^0 has larger value in HH-polarization, the difference between σ_{veg}^0 in two polarization modes is in the range of 3.2 to 3.6 dB. However, the value of σ_{veg}^0 is small (see in Figure 9 (b)). The main contributor of σ_{tot}^0 is $\gamma^2\sigma_{soil}^0$ (see in Figure 9 (a) and (d)).

When the incident angle becomes higher, to 35°, the situation is not similar to what we obtained at 15°. As shown in Figure 10 (d), σ_{soil}^0 at HH and VV-polarization modes simulated by IEM has an obvious difference even from the beginning of the growth period. This difference is up to 1.0 dB. However, larger σ_{soil}^0 is still obtained at VV-polarization, which is the as what we found at 15°. Compare Figure 10 (c) with (d), σ_{soil}^0 is larger than $\gamma^2\sigma_{soil}^0$ at both VV- and HH-polarization as expected. However, this difference is not obvious and only in the range of less
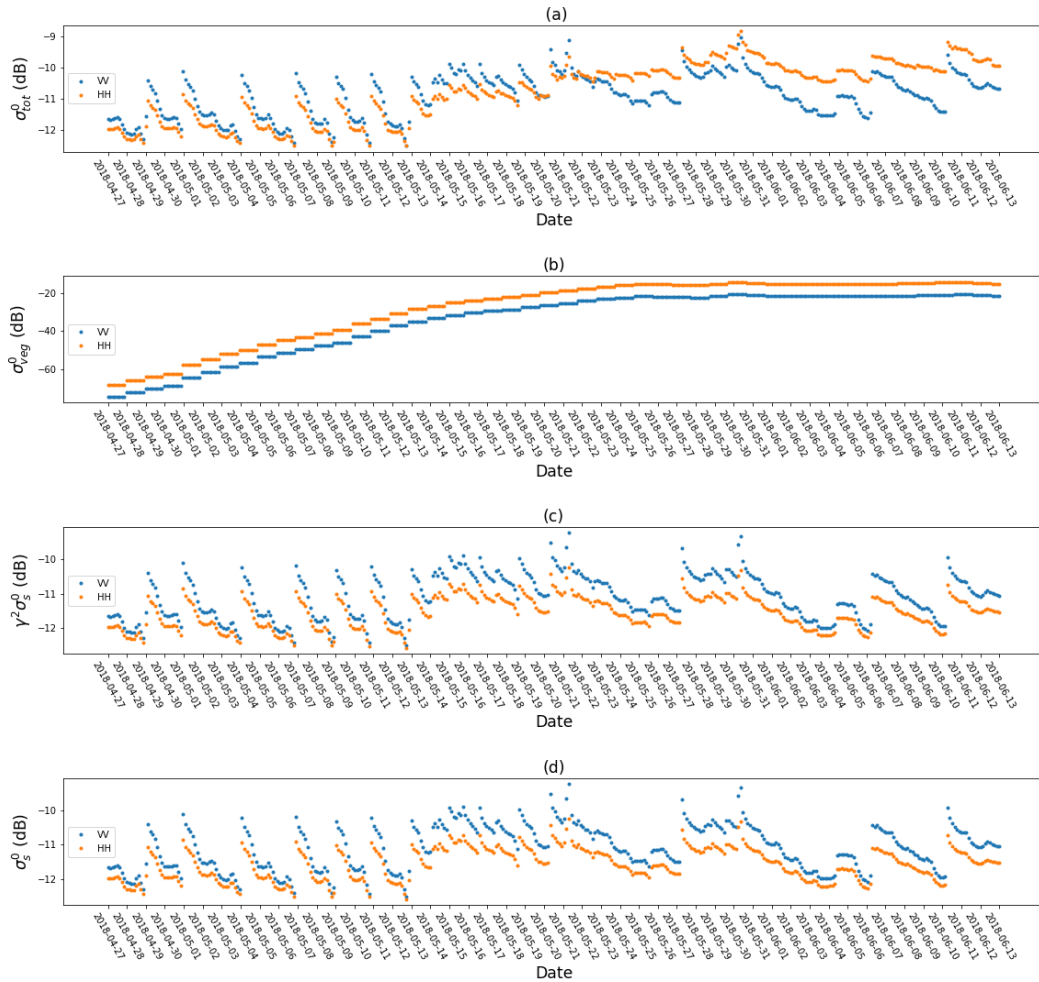

Figure 10 Modeled radar backscatter time series at horizontally and vertically polarized C-band (5.3 GHz) and 35° incident angle using Joseph et al. [4]: (a) total backscatter, (b) vegetation backscatter, (c) attenuated soil backscatter, (d) bare soil backscatter.

than 0.003 dB (both in VV- and HH-polarization), which can be neglected. Recall the results

obtained in Figure 4 (e) and Figure 5 (e), the same result can be obtained that variation of bulk VWC has a very small impact on $\gamma^2\sigma_{soil}^0$ at both VV- and HH-polarization. Then, for the variation of direct backscatter from vegetation, as shown in Figure 10 (b), σ_{veg}^0 has larger value at HH-polarization and the value increases as the plant grows. However, with increasing incident angle, the difference of σ_{veg}^0 at VV- and HH-polarization becomes larger, which is up to 6.5 dB. For variation of σ_{tot}^0, as shown in Figure 10 (a), before 2018-05-17, σ_{tot}^0 at both VV- and HH-polarization are more dominated by $\gamma^2\sigma_{soil}^0$, after that, the difference between VV- and HH-polarization becomes smaller, and finally, around 2018-05-22, σ_{tot}^0 at HH-polarization exceeds the σ_{tot}^0 at VV-polarization. Although, VV-polarization also shows an increasing trend after that day, the increasing trend is not that obvious compared with HH-polarization. This situation means that as the bulk VWC exceeds 3 kg/m^2 (bulk VWC at 2018-05-22), the impact from σ_{veg}^0 is more obvious on σ_{tot}^0, especially for HH polarization.

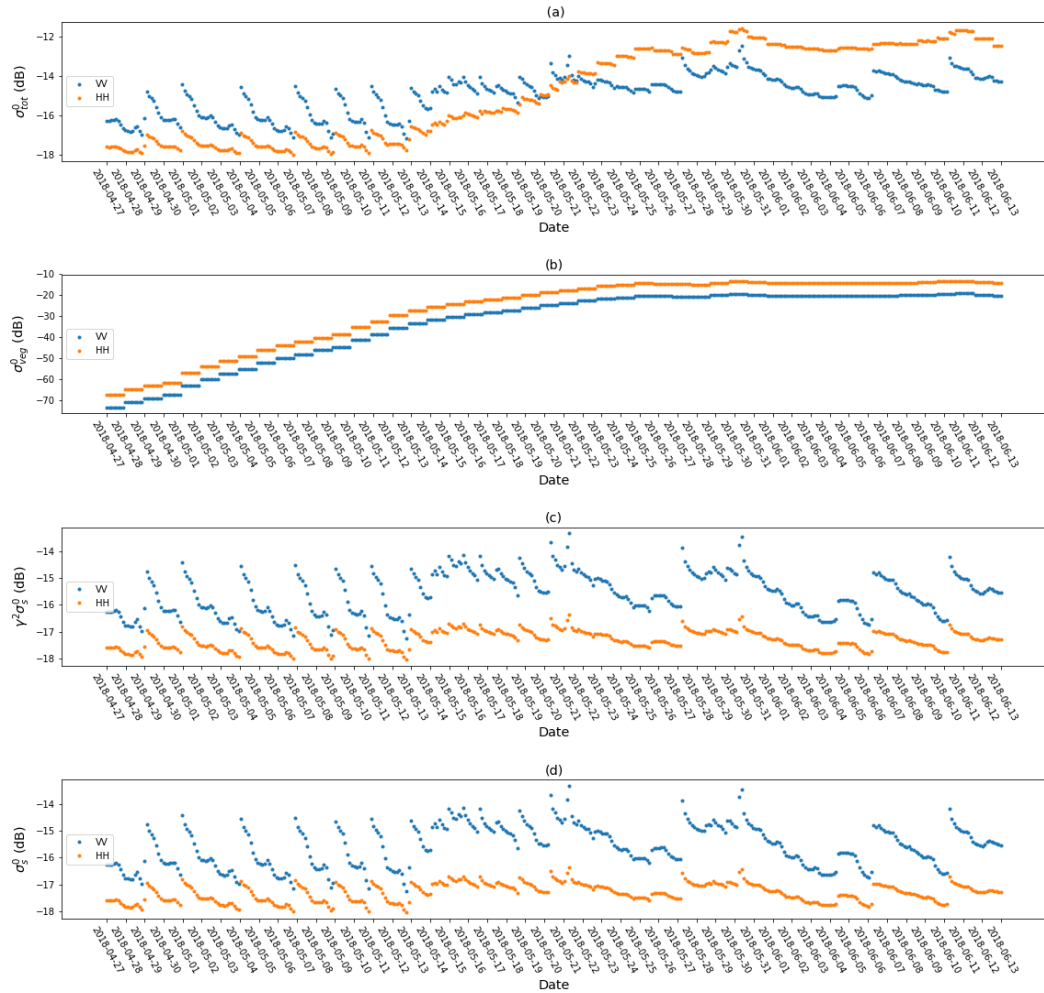Similar results are obtained as the incident angle increase to 55°. In Figure 11 (c) and (d), the

Figure 11 Modeled radar backscatter time series at horizontally and vertically polarized C-band (5.3 GHz) and 55° incident angle using Joseph et al. [4]: (a) total backscatter, (b) vegetation backscatter, (c) attenuated soil backscatter, (d) bare soil backscatter.

difference between σ_{soil}^0 and $\gamma^2\sigma_{soil}^0$ is in the range of less than 0.01 dB (HH), 0.006 dB (VV)

respectively. Therefore, the impact of bulk VWC has very small impact on $\gamma^2\sigma_{soil}^0$. Recall the same result obtained in Figure 4 (f) and Figure 5 (f). Besides, both σ_{soil}^0 and $\gamma^2\sigma_{soil}^0$ have larger value at VV-polarization, the difference of $\gamma^2\sigma_{soil}^0$ between two polarization modes is in the range of 0.8 to 3.0 dB. Thus, increasing incidence angle has more impact on $\gamma^2\sigma_{soil}^0$ at HH-polarization mode. Then, as shown in Figure 11 (b), σ_{veg}^0 at HH-polarization has larger value, the difference of σ_{veg}^0 at two polarization mode is 6.0 dB. For σ_{tot}^0, the increasing trend after 2018-05-22 is more obvious in both VV- and HH-polarization mode, compared with smaller incident angle, especially for HH-polarization. This means σ_{veg}^0 shows more impact on the variation of σ_{tot}^0.

3)   Ulaby et al.(1984):

Figure 12 shows the time series of backscatter simulated with (9)-(13) at X-band, 50° incident angle and VV polarization. The parameter set is derived by Ulaby et al. (1984) and is listed in table 1 as well. V_1, V_2 in Figure 12 is leaf water content and stalk water content respectively. In Figure 12 (d), σ_s is modeled by Dubois's method, and varies in the range of σ_{soil}^0 -17.0 to -13.2 dB under the influence of soil moisture variation. Figure 12 (c) shows the impact of vegetation cover to σ_{soil}^0, this time the impact is divided by canopy layer and stalk layer.
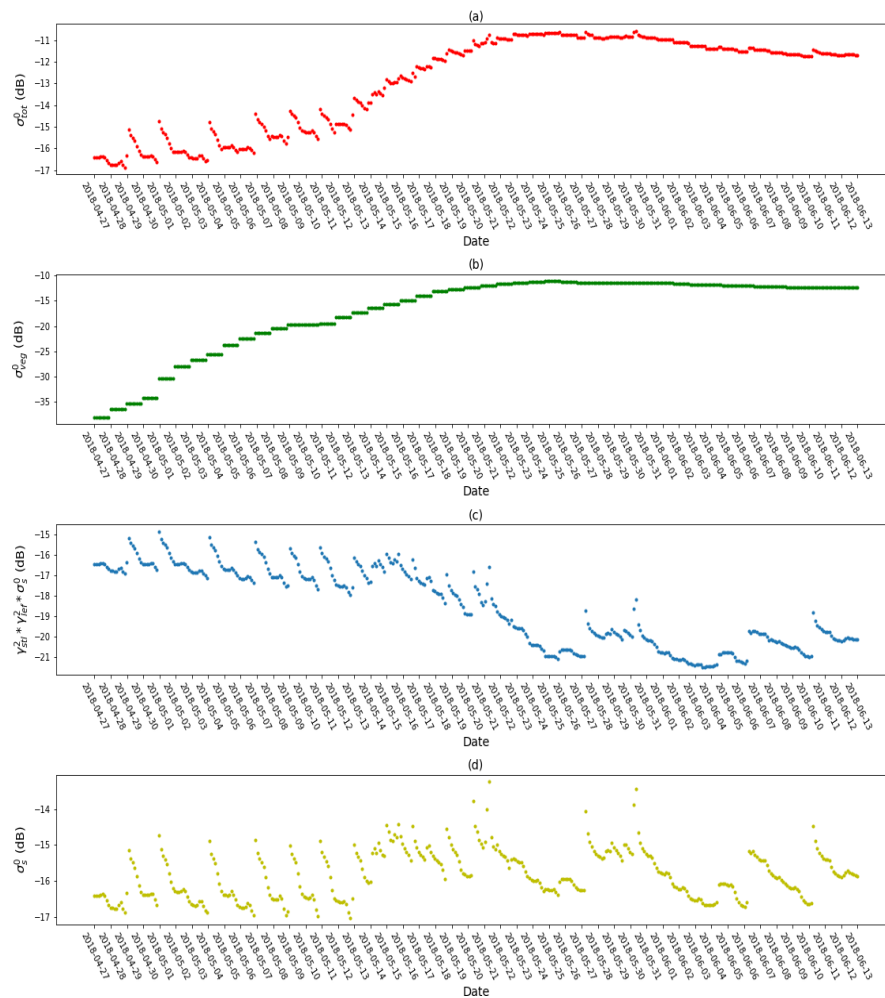

Figure 12 Modeled time series of vegetation and attenuated soil contributions to total radar backscatter at 9.6 GHz (VV, 50◦) using Ulaby et al. [5]: (a) total backscatter, (b) vegetation backscatter, (c) attenuated soil backscatter, and (d) bare soil backscatter. (V_1: leaf water content, V_2: stalk water content)

$\gamma_{lef}^2 \gamma_{stl}^2 \sigma_{soil}^0$ is smaller than σ_{soil}^0 as expected and varies in the range of -21.5 dB to -14.9 dB. The difference between σ_{soil}^0 and $\gamma_{lef}^2 \gamma_{stl}^2 \sigma_{soil}^0$ becomes more obvious at the late growth period as the bulk VWC increases, which is in the range up to 5.0 dB. σ_{veg}^0 change in the range of -38.1 to -11.1 dB, recall the result obtained in Figure 6, backscatter from leaf layer is the main contributor to σ_{veg}^0. As shown in Figure 12 (a), time series of σ_{tot}^0 is similar to that of σ_{veg}^0. Moreover, σ_{veg}^0 is dominated by leaf VWC. Therefore, σ_{tot}^0 is influenced by leaf VWC. Notice in Figure 12 (a), there is a dropping at the late growth period, however, the interval of σ_{veg}^0 is too large, the drop we observed is less obvious. Therefore, cut the small σ_{veg}^0 value at the beginning of the growth period, replot the time series of σ_{veg} in Figure 13 (a). It's more obvious that at the late growth period, variation of σ_{tot}^0 is also similar to that of σ_{veg}^0. This drop is cause by decrease of observed leaf water content (see in Figure 13 (b)).
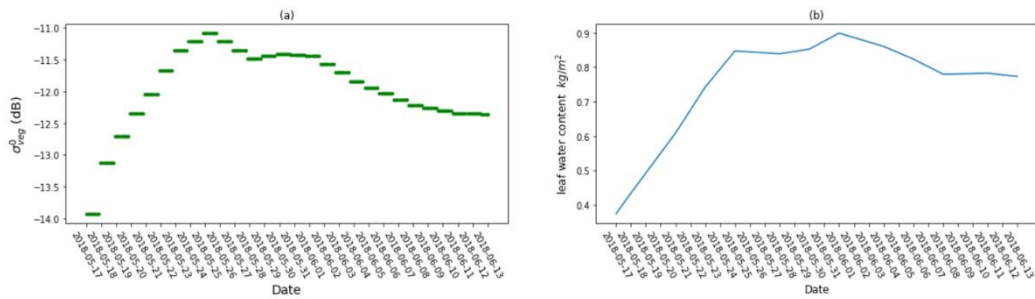

Figure 13 Variation of (a) vegetation backscatter and (b) leaf water content at late growth period

Another time series of backscatter simulated with (9)-(13) at X-band, 50° incident angle and VV polarization is shown in Figure 15. The parameter set is also derived by *Ulaby et al.* (1984) and is listed in table 1. The main difference is that we use canopy leaf area index (LAI) as V_1 instead of leaf layer water content. LAI determines the solar radiation intercepted by canopy and is also an important component of crop yield models [5]. The variation of LAI in growth period is shown in Figure 14.
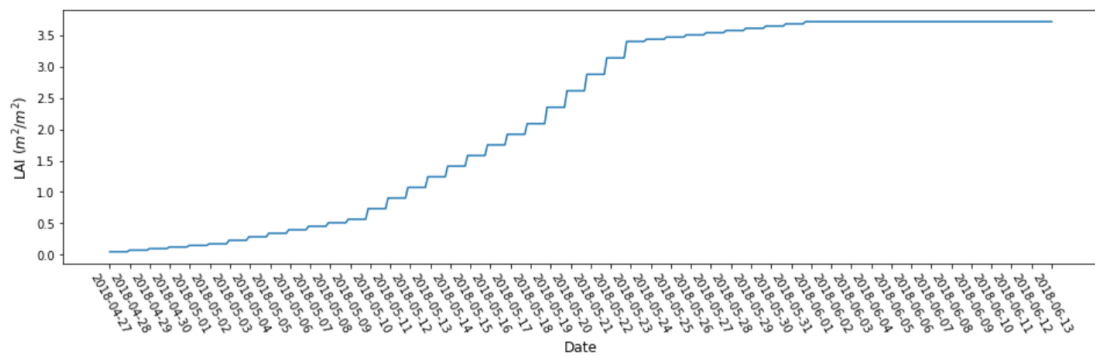

Figure 14 Variation of LAI during the growth period

The time series is similar to what we obtained above. However, at the late growth period in this model, the attenuated soil backscatter has much smaller value and less sensitive to bare soil

backscatter (see in Figure 15 (c)). At higher frequency and larger incident angles, the ability of microwave to penetrate dense vegetation layer becomes weaker.
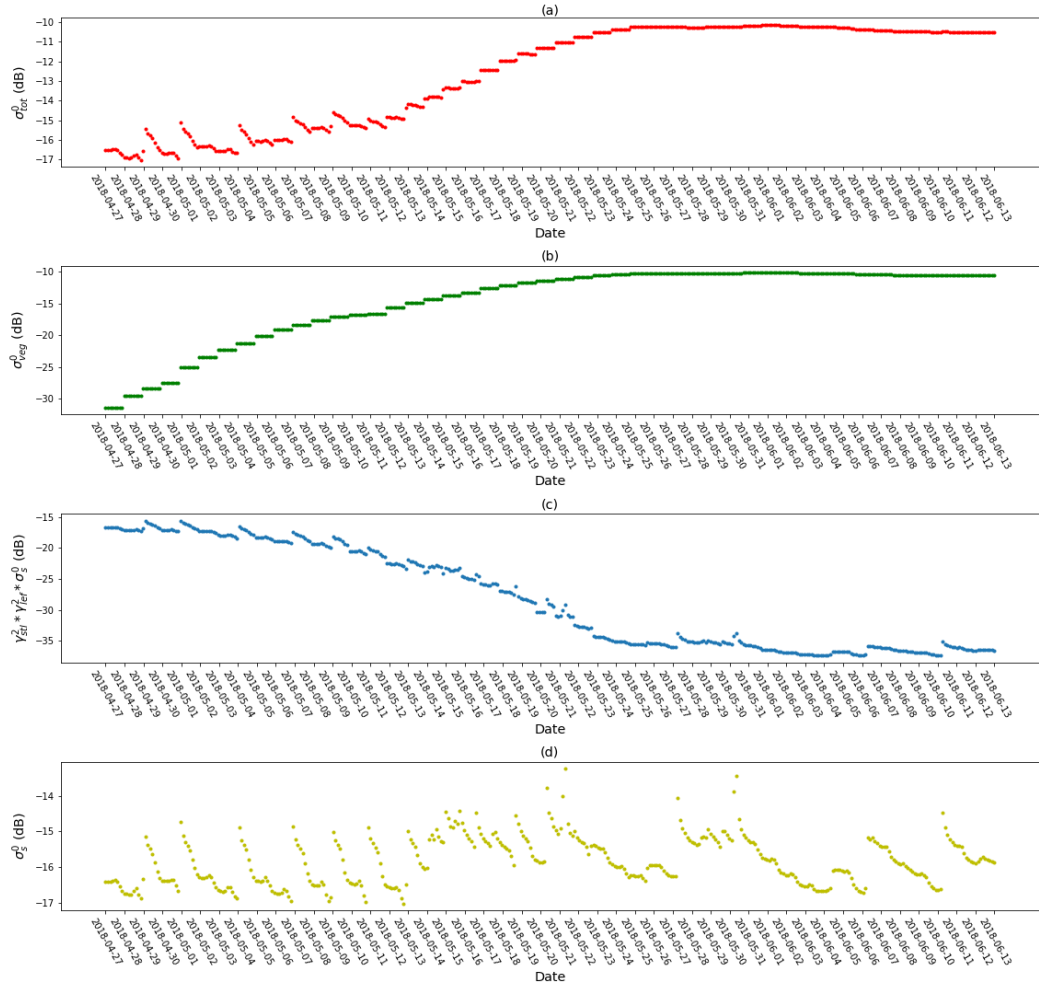

Figure 15 Modeled time series of vegetation and attenuated soil contributions to total radar backscatter at 9.6 GHz (VV, 50◦) using Ulaby et al. [5]: (a) total backscatter, (b) vegetation backscatter, (c) attenuated soil backscatter, and (d) bare soil backscatter. (V_1: LAI, V_2: stalk water content)

As shown in Figure 16, the backscatter from leaf layer provides the majority of σ_{veg}^0. The contribution to σ_{tot}^0 made by $\gamma_{lef}^2 \gamma_{stl}^2 \sigma_{soil}^0$ is important only when LAI is less than 0.5 m^2/m^2.
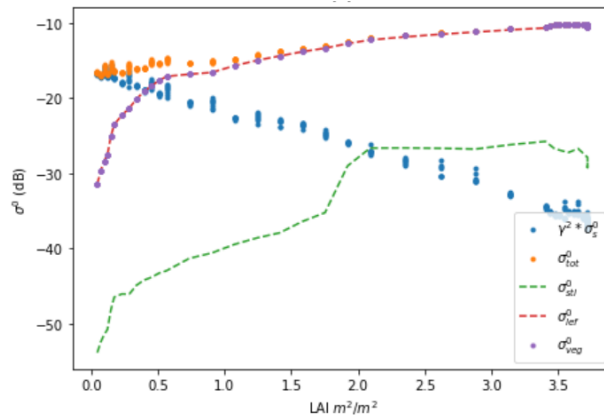
Figure 16 Variation of total backscatter and different contributor of total backscatter as function of

bulk VWC at 9.6 GHz using Ulaby et al. [5].

D. Parameter Derivation

Sentinel-1 is part of Europe's Copernicus program and at the moment has two satellites in orbit, Sentinel-1A and Sentinel-1B launched in April 2014 and 2016, respectively. The Sentinel-1 satellites carry Synthetic Aperture Radars (SAR), providing backscatter at C-band (5.405 GHz). The acquisition mode over (non-polar) land is Interferometric Wide (IW) swath mode. The SAR instruments are designed to provide co- and cross-polarized backscatter over a 250 km swath at a 20 m spatial resolution in single look. The temporal revisit time of one Sentinel-1 satellite is 12 days, and temporal coverage is 1.5–4 days over Europe using both Sentinel-1A and Sentinel-1B [21]. In this research, three backscatter value (2018-05-08, 2018-05-20, 2-18-06-13) from Sentinel 1 is available during the growth period (2018-04-27 to 2-18-06-13). WCM is applied using IEM to simulate the σ_{soil}^0 and the bulk VWC for representing V1 and V2. Then, the vegetation parameters (A and B), are derived by least squares optimization algorithm.

Table 2

Parameter set used in Water Cloud Model

Model	Radar Parameter				Vegetation Parameters		Model Outcome	
	Band	Frequency (GHz)	incident angle	polarization	A	B	RMSD	ρ
Joseph et al. (2010)	C	5.55	39°	VV	17.72	$3.08*10^{-4}$	1.26	0.91

The parameter values, RMSD and ρ are listed in table 2. Further, Figure 17 shows the backscatter from Sentinel 1 and the σ_{tot}^0 simulated by WCM. According to limited data shown in Figure 17, we can see that σ_{tot}^0 simulated by WCM is closer to measured radar backscatter at the later growth period.
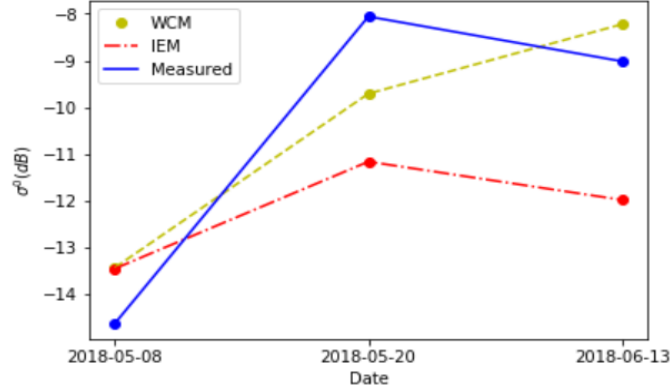

Figure 17 C-band measured, IEM simulated, WCM simulated σo at the day Sentinel 1

passed by the corn field

Then, applied this new parameter set to entire growth period and do sensitivity analysis and time series analysis.

In Figure 18 (a), $\gamma^2\sigma_{soil}^0$ provides the majority part of σ_{tot}^0, when bulk VWC < 3 kg/m^2 (see in Figure 18 (a)). Like what we already notice above, $\gamma^2\sigma_{soil}^0$ is independent to bulk VWC (see in Figure 18 (b)) due to extremely small B value, which leads γ^2 approximately equal to 1. Therefore, the difference between $\gamma^2\sigma_{soil}^0$ and σ_{soil}^0 is very small and this model fails to capture the impact of bulk VWC on $\gamma^2\sigma_{soil}^0$ Figure 19 (c)).
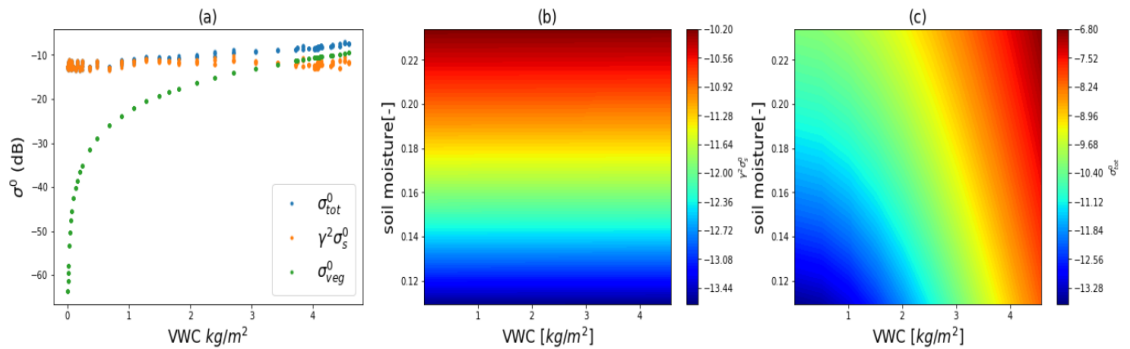

Figure 18 Sensitivity of C-band (5.405 GHz) vertically polarized radar backscatter at different incidence angles using derived parameter: (a) Vegetation and attenuated soil contributions as a function of bulk VWC for 39°, (b) Attenuated soil backscatter as a function of bulk VWC and soil moisture for 39°, (c) Total backscatter as a function of bulk VWC and soil moisture for 39°.

However, the impact of bulk VWC on σ_{tot}^0 is obvious, which is caused by a significantly large A. Therefore, with increasing bulk VWC, $\gamma^2\sigma_{soil}^0$ and σ_{veg}^0, are comparable in magnitude and both influence σ_{tot}^0. When σ_{veg}^0 exceeds $\gamma^2\sigma_{soil}^0$ around bulk VWC = 3 kg/m^2, σ_{veg} plays a more important role in σ_{tot}^0. Thus, the variation of σ_{tot}^0 mainly reflects the variation of $\gamma^2\sigma_{soil}^0$ at the beginning of the growth cycle. Then, at latter growth period, the influence from

σ_{veg}^0 becomes more obvious which leads to the increase of σ_{tot}^0 (see in Figure 19 (a)). Besides, σ_{tot}^0 is less sensitive at larger bulk VWC (see in Figure 18 (c)).
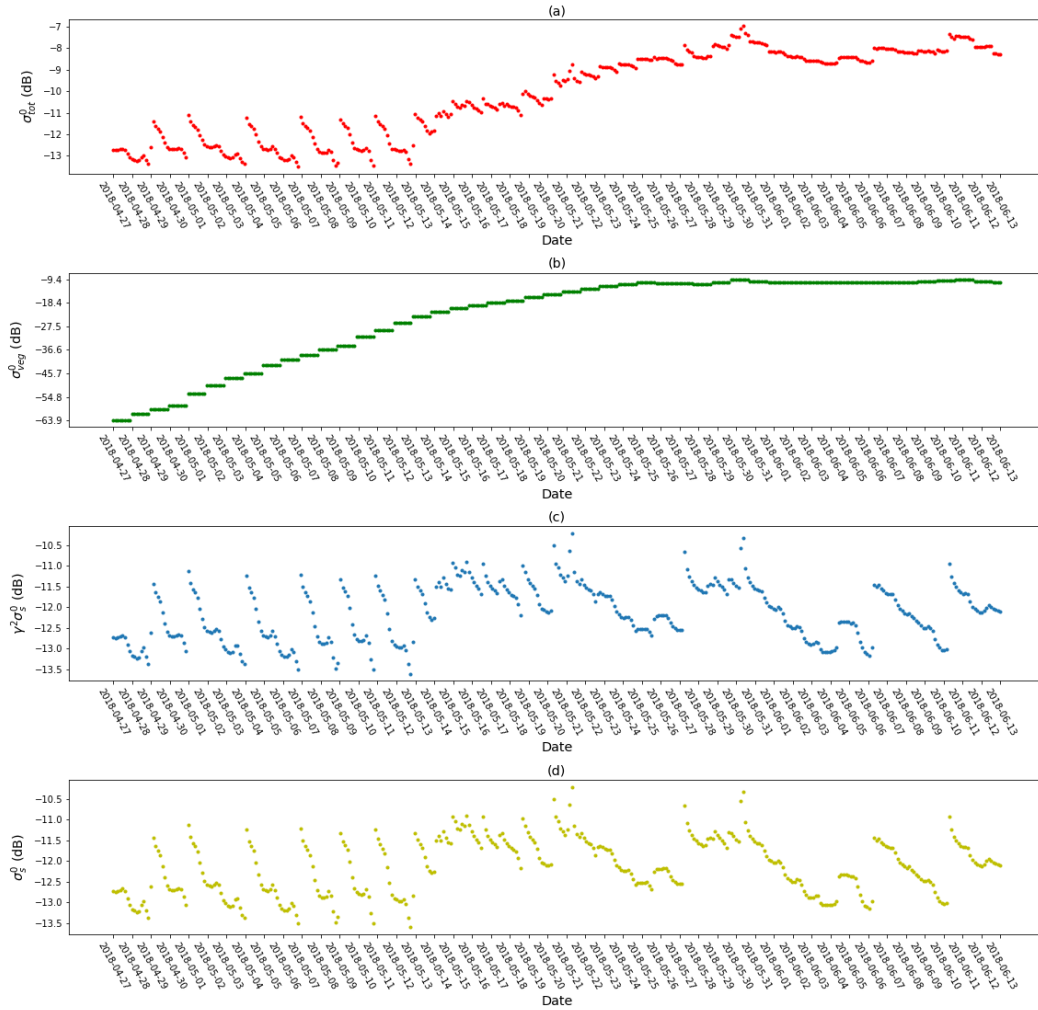

Figure 19 Modeled radar backscatter time series at horizontally and vertically polarized C-band (5.405 GHz) and 39° incident angle using derived parameter: (a) total backscatter, (b) vegetation backscatter, (c) attenuated soil backscatter, (d) bare soil backscatter

V. Conclusion

In this paper, we investigated the impact of soil moisture and bulk VWC variations on radar backscatter at different radar parameters in the maize canopy through entire growth period. A Water-Cloud model based on three published studies was used to simulate the radar backscatter. The radar parameters are different at a range of frequencies, incident angles and polarization modes. From ground measurement, bulk VWC varies from 0 to 4.6 kg/m^2 and soil moisture varies from 0.11 to 0.23 m^3/m^3 in the growth period.

Results shows that, at high frequency and large incident angles, σ_{tot}^0 is influenced by both bulk VWC and soil moisture. However, variation in bulk VWC shows more impact on σ_{tot}^0. At C-band, this phenomenon is more obvious at HH-polarization mode. Besides, at X-band, a double layer WCM shows that even though the majority of bulk VWC is from stalk layer, backscatter from leaf layer is the main part of σ_{veg}^0 and also influence σ_{tot}^0. Sensitivity analysis shows that an increase of bulk VWC

can cause a decrease of σ_{tot}^0 when $\gamma^2 \sigma_{soil}^0$ is the dominated contributor at small incident angle. However, an increase of bulk VWC can also cause an increase of σ_{tot}^0 when the influence of σ_{veg}^0 becomes more important at larger incident angle.

VI. Reference

[1] A. K. Fung, Z. Li, and K. S. Chen, "Backscattering from a randomly rough dielectric surface," *IEEE Trans. Geosci. Remote Sens.*, vol. 30, pp. 356−369, Mar. 1992.

[2] P. C. Dubois, J. van Zyl, and T. Engman, "Measuring soil moisture with imaging radars," *IEEE Trans. Geosci. Remote Sens.*, vol. 33, no. 4, pp. 915–926, Jul. 1995.

[3] K. Dabrowska-Zielinksa, Y. Inoue, W. Kowalik, and M. Gruszcynska, "Inferring the effect of plant and soil variables on C- and L-band SAR backscatter over agricultural fields, based on model analysis," *Adv. Space Res.*, vol. 39, no. 1, pp. 139–148, Jan. 2007.

[4] A. Joseph, R. van der Velde, P. O'Neill, R. Lang, and T. Gish, "Effects of corn on C- and L-band radar backscatter: A correction method for soil moisture retrieval," *Remote Sens. Environ.*, vol. 114, no. 11, pp. 2417–2430, Nov. 2010.

[5] F. T. Ulaby, C. Allen, G. Eger, and E. Kanemasu, "Relating the microwave backscattering coefficient to leaf area index," *Remote Sens. Environ.*, vol. 14, no. 1–3, pp. 113–133, Jan. 1984.

[6] Y.Oh, K. Sarabandi, F.T.UIaby, "An empirical model and an inversion technique for radar scattering from bare soil surface," *IEEE Trans. Geosci. Remote Sens.*, vol. 30, pp. 370-381, 1992.

[7] M. S. Dawson, A. K. Fung and M. T. Manry, "A robust statistical-based estimator for soil moisture retrieval from radar measurements," *IEEE Trans. Geosci. Remote Sens.*, vol. 35, no. 1, pp. 57-67, Jan.1997

[8] F. T. Ulaby, P. P. Batlivala and M. C. Dobson, "Microwave Backscatter Dependence on Surface Roughness, Soil Moisture, and Soil Texture: Part I-Bare Soil," *IEEE Trans. Geosci. Remote Sens.*, vol. 16, no. 4, pp. 286-295, Oct. 1978.

[9] F. T. Ulaby, R. More, and A. Fung, "Microwave Remote Sensing: Active and Passive, Vol. II.," Boston, MA, USA: Artech House, 1986

[10] K. S. Chen, T. Wu, L. Tsang, Q. Li, J. Shi and A.K. Fung, "Emission of rough surfaces calculated by the integral equation method with comparison to three-dimensional moment method simulations," *IEEE Trans. Geosci. Remote Sens.*, vol. 41, no. 1, pp. 90-101, Jan. 2003.

[11] S. C. Steele-Dunne, H. McNairn, A. Monsivais-Huertero, J. Judge, P. Liu and K. Papathanassiou, "Radar Remote Sensing of Agricultural Canopies: A Review," *IEEE Journal of Selected Topics in Applied Earth Observations and Remote Sensing.,* vol. 10, no. 5, pp. 2249-2273, May. 2017.

[12] R. D. De Roo, Y. Du, F. T. Ulaby, and M. C. Dobson, "A semi-empirical backscattering model at L-band and C-band for a soybean canopy with soil moisture inversion," *IEEE Trans. Geosci. Remote Sens*, vol. 39, no. 4, pp. 864−872, Apr.2001.

[13] J. Wen, Z. Su, "The estimation of soil moisture from ERS wind scatterometer data over the Tibetan plateau," *Physics and Chemistry of the Earth, Parts A/B/C*, vol. 28, pp. 53−61, 2003.

[14] Z. Bartalis, W. Wagner, V. Naeimi, S. Hasenauer, L. Scipal, H. Bonekamp, J. Figa and C. Anderson, "Initial soil moisture retrieval from Metop-A advanced scatterometer," *Geophysical Research Letters*, vol. 34, 2007.

[15] U. Narayan, V. Lakshmi and T. J. Jackson, "High-resolution change estimation of soil moisture using L-band radiometer and radar observations made during the SMEX02 experiments," *IEEE Trans. Geosci. Remote Sens*, vol. 44, np. 6, pp. 1545−1554, Jun.2006.

[16] J. Alvarez-Mozos, J. Casali, M. Gonzalez-Audicana, and N. E. C. Verhoest, "Assessment of the operational applicability of RadarSat-1 data for surface soil moisture estimation," *IEEE Trans. Geosci. Remote Sens*, vol. 44, no. 4, pp. 913−924, Apr.2006.

[17] N. E. C. Verhoest, P. A. Troch, C. Paniconi and F. P. De Troch, "Mapping basin scale variable source areas from multitemporal remotely sensed observations of soil moisture behavior," *Water Resources Research*, vol. 34, pp. 3235−3244, 1998.

[18] E. Attema and F.T. Ulaby, "Vegetation modeled as a water cloud," *Radio Sci.,* vol. 13, no. 2, pp. 357–364, Mar./Apr.1978.

[19] T. van Emmerik, S. C. Steele-Dunne, J. Judge and N. van de Giesen, "Impact of Diurnal Variation in Vegetation Water Content on Radar Backscatter From Maize During Water Stress," *IEEE Trans. Geosci. Remote Sens*, vol. 53, no. 7, pp. 3855−3869, Jul.2015.

[20] F.T. Ulaby, "Radar response to vegetation," *IEEE Trans. Antennas Propag.*, vol. 23, no. 1, pp. 36–45, Jan. 1975.

[21] M. Vreugdenhil, W. Wagner, B. Bauer-Marschallinger, I. Pfeil,I. Teubner,C. Rüdiger and P. Strauss, "Sensitivity of Sentinel-1 Backscatter to Vegetation Dynamics: An Austrian Case Study," *Remote Sens.,* vol. 10, 2018.